

# Implementation and Performance of the Electronics and Computing System of the Gamma Ray Energy Tracking In-Beam Nuclear Array (GRETINA)

Sergio Zimmermann, *Senior Member, IEEE*, John T. Anderson, Dionisio Doering, *Member, IEEE*, John Joseph, Carl Lionberger, *Member, IEEE*, Thorsten Stezelberger, and Harold Yaver

**Abstract**—The Gamma Ray Energy Tracking In-Beam Nuclear Array (GRETINA), a germanium detector system capable of measuring energy and position (within better than 2 mm rms) of gamma-ray interaction points and tracking multiple gamma-ray interactions, has been built. GRETINA is composed of seven detector modules, each with four high purity germanium crystals. Four custom designed electronics support the operation of the detectors: Digitizer/Digital Signal Processing (DSP), Trigger/Timing, Breakout Chassis and the Detector Interface Box. The Digitizer/DSP converts the analog information with 14-bit analog to digital converters operating at 100 MS/s, and digitally processes the data to determine the energy and timing information of the gamma interactions within a crystal. The computing system is composed of VME readout CPUs running VxWorks, which communicate with 62 dual-processor farm (each processor with four cores) through a 10 Gb/s Ethernet switch. The CPUs read out the digitizer/DSPs and send the data to the farm. The processors compute the position and track of the interactions of the gamma-ray inside the crystals. The processor farm is capable of processing in real-time the position of 20 000 gamma-rays/s. In this paper we will present the details of the implementation and performance of the electronics and computing system of GRETINA.

**Index Terms**—Data acquisition systems, digital signal processing, gamma-ray spectrometer, trigger systems.

## I. INTRODUCTION

**G**AMMA-RAYS emitted by nuclei in their de-excitation process to their ground states are unique probes to study elementary modes of excitation of the atomic nucleus and their properties. Thus, gamma-ray spectroscopy plays a major role in this research, particularly in the characterization of the single particle and collective degrees of freedom.

As is generally the case in all areas of science, development of new detectors and techniques have deepened our knowledge of nuclei and their properties and almost always led to discoveries of new and unexpected phenomena.

Manuscript received November 21, 2011; revised May 08, 2012; accepted May 27, 2012. Date of publication August 27, 2012; date of current version October 09, 2012. This work was supported by the Director, Office of Science of the U.S. Department of Energy under Contract DE-AC02-05CH11231.

S. Zimmermann, D. Doering, J. Joseph, C. Lionberger, T. Stezelberger, and H. Yaver are with the Lawrence Berkeley National Laboratory, Berkeley, CA 94720 USA (e-mail: szimmermann@lbl.gov).

J. T. Anderson is with Argonne National Laboratory, Argonne, IL 60439 USA.

Digital Object Identifier 10.1109/TNS.2012.2205587



Fig. 1. GRETINA detector module.

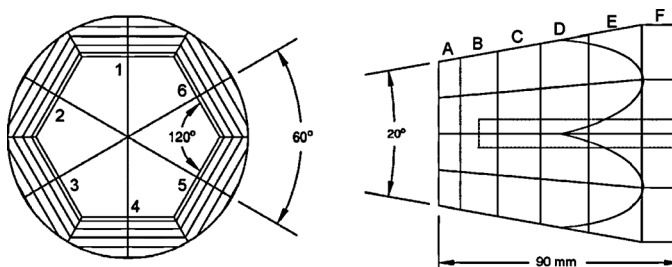


Fig. 2. Sketch of the segmentation of the Ge detector.

The Gamma Ray Energy Tracking In-Beam Nuclear Array (GRETINA) is a first implementation of a new detector array system based on gamma-ray tracking. In GRETINA, this technique of gamma-ray tracking is capable of measuring the energy and position (within better than 2 mm rms) of each gamma-ray interaction point and track multiple gamma-ray interactions. These new arrays have substantially improved efficiency and effective resolution, potentially increasing the resolving power of gamma-ray spectroscopy by two orders of magnitude from current generation arrays [1], [2].

GRETINA is composed of seven detector modules, each with four high purity segmented germanium crystals (Fig. 1). Every crystal is a cylinder with flat tapered shape (Fig. 2), with segments deposited on the surfaces forming a matrix of  $6 \times 6$  longitudinal and transverse segments. Each segment is identified using sequential alphanumeric characters: A to F for longitudinal position and 1 to 6 for transverse position, with the letter A corresponding to the segment ring on the front of the detector (the portion that is tapered).

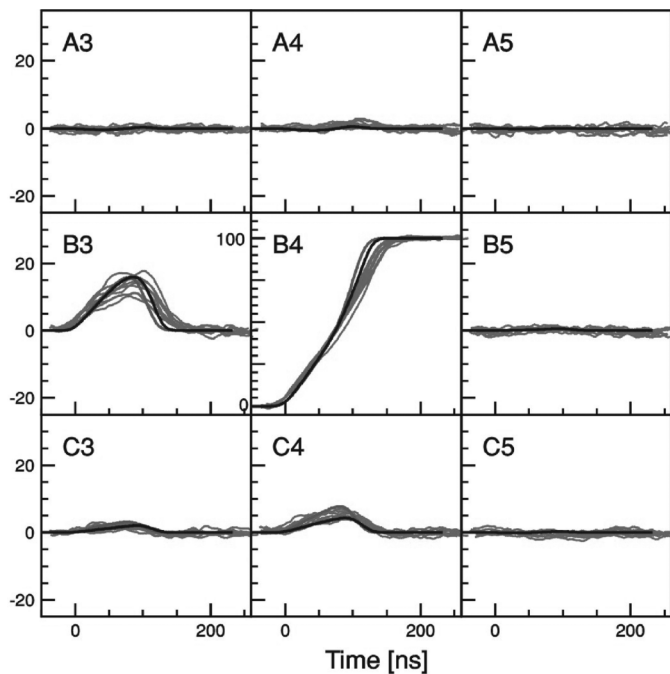


Fig. 3. Waveforms for interactions below segment B4.

The gamma ray interacts with the germanium crystal and induces charge on the segments and central contact. The crystal is at approximately  $-174^{\circ}\text{C}$ . The charge sensitive amplifier integrates this charge and drives an analog voltage to the GRETINA front-end electronics. Fig. 3 shows examples of nine typical waveforms on the segments of the detector. The gamma-rays are interacting with the detector at a specific location below the B4 segment. The segments shown are the one that collects the charge (B4) and its eight nearest neighbors. The neighbors detect induced charge. A total of 16 measured shapes are plotted in gray and the calculated waveforms for this given position are plotted in black. Observe that the measured signals include noise.

The seven GRETINA detector modules are supported by a mechanical structure composed of two quasi-hemispheres that surround the target chamber (Fig. 4). The quasi-hemispheres are capable of supporting up to 21 detector modules. The structure allows rotation for detector mounting (through a gear box in the end of the axles) and translation to access the target chamber (through railroad cars). Hexapods connect the structures to the railroad cars. Fig. 4 shows a sketch of the support structure, with all possible positions instrumented with a detector module. Fig. 5 shows five detector modules assembled on the support structure, adjacent to the beam-line. There are plans to construct the full  $4\text{-}\pi$  detector module array, GRETA [4], and the electronics system foresees this possible scenario.

In this paper, the implementation and performance of the electronics and computing system for GRETINA will be presented, including some significant results of the engineering runs.

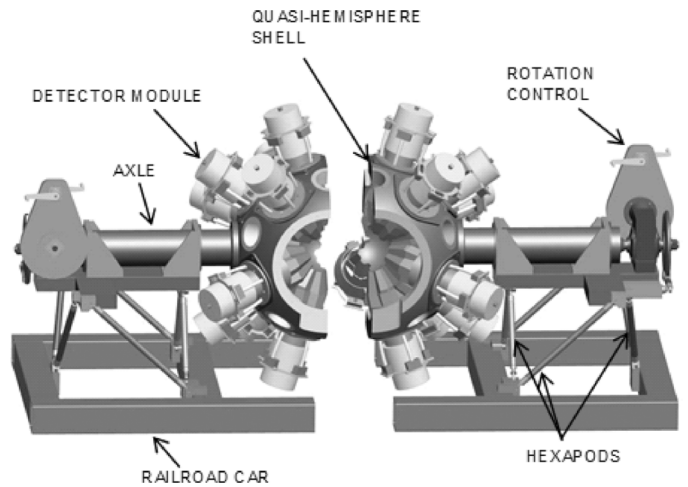


Fig. 4. GRETINA mechanical support structure.

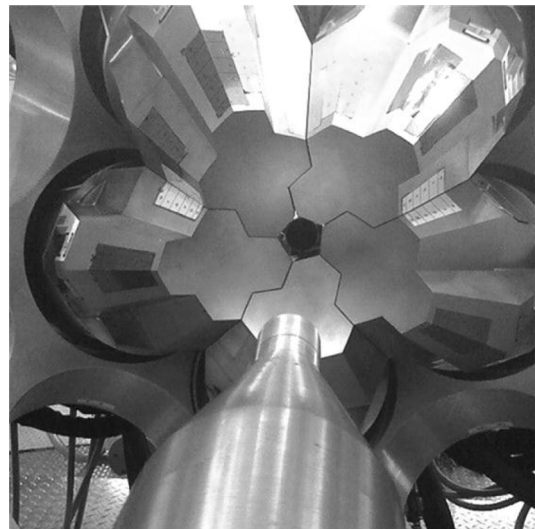


Fig. 5. Five detectors mounted on the support structure.

## II. ELECTRONIC SYSTEMS

Fig. 6 shows a block diagram of the GRETINA electronics [5] and computing system. The oblong shape on the left represents the detector modules and its crystals. Charge sensitive pre-amplifiers are connected to custom made Digitizer/Digital Signal Processing (DSP) VME modules. These pre-amplifiers employ resistive feedback. The Trigger, Timing and Control (TTC) unit provides high-speed triggers, synchronized clock and controls to the digitizers and, optionally, to auxiliary detectors. Fig. 7 shows a photograph of the Digitizers/DSP, TTC and power supplies (PS) crate in the electronics shack.

### A. Electronics Hardware

The Digitizer/DSP modules and the TTC, together with Breakout Chassis, Detector Interface Box and PS form the GRETINA electronics (Fig. 8). Four digitizers instrument one crystal; each master digitizer interfaces with the TTC system and controls the three other slave digitizers.

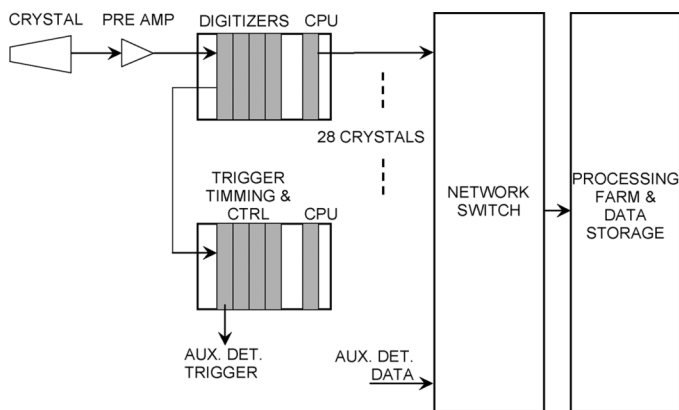


Fig. 6. GREYINA electronics and computing systems.

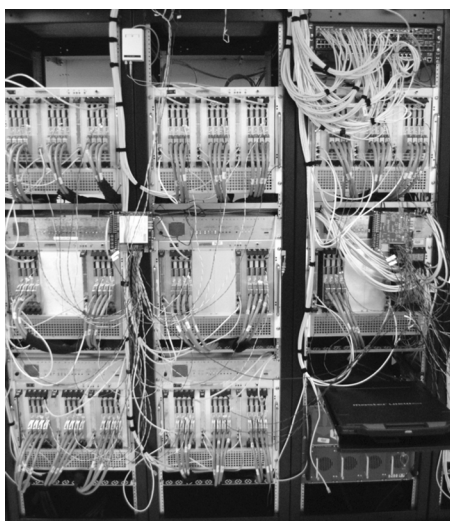


Fig. 7. Digitizers and trigger systems installed in the electronics shack.

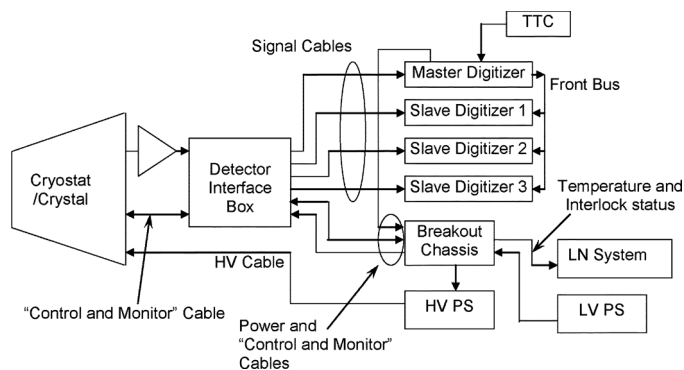


Fig. 8. Electronics hardware block diagram.

The Digitizer/DSP module samples the segment and central contact analog information using 14-bit analog to digital converters (ADC) operating at 100 MS/s. The ADC used was an AD645 from Analog Devices. The ADCs are connected to a field programmable gate array (FPGA), which digitally processes the conversions. The Digitizer/DSPs communicates with

the TTC system through a bidirectional gigabit (Gb) link to exchange trigger information. The trigger system issues commands related to the events that met the trigger criteria to the digitizers through these same Gb links. A digital bus on the front panel allows the digitizers serving a crystal to synchronize among themselves for clock and trigger information. The master digitizer controls the operations on the bus by enabling transactions synchronously with a 50 MHz clock. It addresses each digitizer separately (with a two bit address) or broadcast operations to all digitizers (e.g., trigger information). When the TTC issued a trigger, the events are stored in a FIFO in the Digitizer/DSP modules. Later on, the VME readout CPUs in the digitizer crates poll and read out the data from each digitizer FIFO and send to the processor farm. Four trigger algorithms have been implemented: multiplicity, energy, pattern distribution and auxiliary detector trigger. For more details on these algorithms refer to [5].

The GREYINA Digitizer/DSP module communicates with the system host computer using the VME64x protocol, implemented in a custom LBNL designed FPGA, and supports A32/D32 address and data format for block transfers and single read/write access only. VME Slave Interface required intensive optimization of 2 FPGA designs to accommodate the large volume of event data transferred from the detector digitizers to the host processing system within the allotted system data bandwidth. The final VHDL implementation resulted in a sustained transfer rate of 18 MB/s of triggered event data for each DSP/Digitizer.

The Detector Interface Box interfaces the detector with the rest of the GREYINA electronics. It distributes the pre-amplifier signals to the DSP/Digitizer modules using four 18 m cables, each with 10 twisted shielded pairs inside to decrease crosstalk. One power cable powers up the amplifiers and monitoring hardware inside the detector and one control and monitor cable complete the interface with the electronics. The Detector Interface Box also has analog and digital circuitry that injects charge in the input of the amplifiers for testing and calibration. The functions of this circuitry are controlled by digital outputs of the master digitizers through a slow speed serial protocol and a charge-inject control line.

The Breakout Chassis (BC) serves a detector module (Fig. 8). The detector has an interlock output to protect the Ge crystals and pre-amplifiers if the crystal warms up or the pre-amplifier low voltage (LV) fails. The BC interfaces this interlock output with the enable/disable control input of the high voltage (HV) bias floating supplies of each crystal. The BC also monitors the temperature of the Ge crystals and pre-amplifier compartments and interfaces these signals with the liquid nitrogen (LN) system. These temperatures are used as part of the automatic LN filling system, as well as for alarms and limits and trending reports. The BC isolates the detector ground of all these functions (including charge inject) from the rest of the electronics. Finally, the BC also adapts the connectors of the pre-amplifiers LV floating power supplies (PS) and the Detector Interface Box.

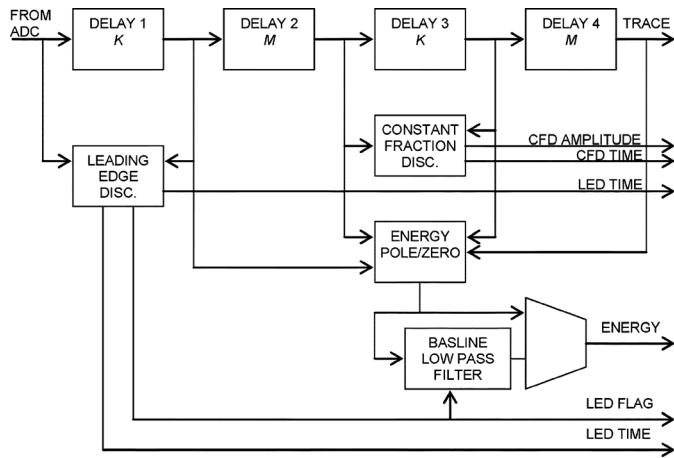


Fig. 9. Digital signal processing.

### B. Digital Signal Processing

Fig. 9 shows a block diagram of the digital processing algorithms and how they are interconnect and Table I describes the algorithms. The processing is optimized to be implemented using the internal FPGA resources and occurs at a clock rate of 100 MHz. This results in approximately 25 giga-operations/s. While the processing occurs, the raw data is stored in 10  $\mu$ sec circular buffers (designed around the FPGA block RAMs). The pole/zero (PZ) cancellation algorithm compensates the transfer function of the detector resistive-feedback amplifier, where  $\tau$  is the time constant of the amplifier output (a differentiator of approximately 60  $\mu$ s fall time). The baseline restoration (BL) algorithm is implemented as a gated low pass filter at the output of the trapezoidal filter. Its time constant is set to be longer than  $\tau$  to restore low frequency variation on the baseline. By gating the BL filter we avoid distortions to its signal value when an incoming pulse caused by a gamma ray interaction in the detector is being processed. The gating starts with the leading edge discriminator signal and is extended for a period longer than the time of the trapezoidal filter. For further details on these algorithms refer to [6].

Fig. 10 illustrates the impact of the selection of the PZ  $\tau$  parameter on the full width at half maximum (FWHM) energy resolution performance. As one can observe, careful tuning of this parameter properly compensates the time constant of the amplifier. Presently, the PZ and BL restoration are working well for operations of up-to 30 Kevents/s in each segment.

## III. COMPUTING SYSTEMS

The computing system is composed of readout CPUs communicating with 62 Linux-based dual-processor farm (each processor with four cores) through a 10 Gb/s Ethernet switch (Fig. 6). The DAQ and control systems are highly distributed and are capable of performing compute-intensive tasks during data acquisition. Fig. 11 gives an overview of the major elements of the software. This diagram represents the full deployment of the system, in which raw data is acquired by the digitizers and is processed by the signal decomposition (SD) algorithm to determine interaction energy  $E$ , position  $r$ ,  $\theta$ ,  $z$  (within better than

 TABLE I  
DIGITAL SIGNAL PROCESSING

#### Leading Edge Discrimination

$$y(n) = x(n) - x(n-k) \text{ (differentiation)}$$

$$y(n) = (x(n) + x(n-2)) + x(n-1) \lll 1 \text{ (}\times 4, \text{ Gaussian filtering)}$$

Threshold comparison  $\rightarrow$  LE discriminator time

#### Constant Fraction Discrimination

$$y(n) = x(n) - x(n-k) \text{ (differentiation)}$$

$$y(n) = (x(n) + x(n-2)) + x(n-1) \lll 1 \text{ (}\times 2, \text{ Gaussian filtering)}$$

$$y(n) = x(n-k) \lll ab - x(n) \text{ (constant fraction)}$$

Zero crossing comparison  $\rightarrow$  CFD time

#### Trapezoidal filter and energy determination [7]

$$y(n) = y(n-1) + ((x(n) + x(n-2m-k)) - (x(n-m) + x(n-m-k)))$$

Maximum tracking  $\rightarrow$  energy

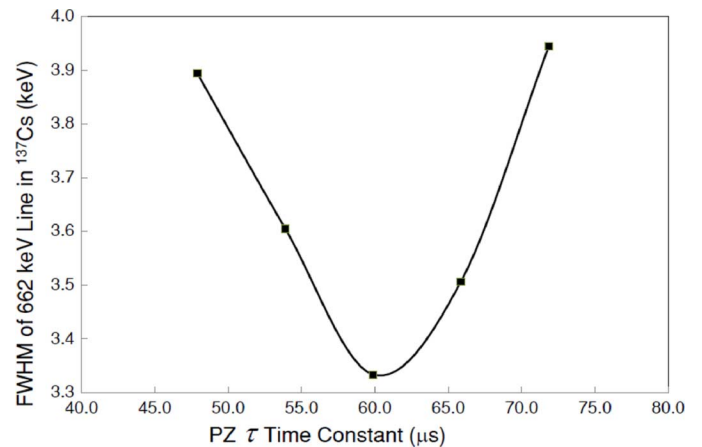
#### Pole-Zero cancellation

$$I(n) = I(n-1) + x(n)$$

$$y(n) = x(n) + I(n)/\tau \text{ (where } \tau \text{ is the amplifier time constant)}$$

#### Baseline restoration

$$BL(n) = BL(n-1) + k * [x(n) - BL(n)], \text{ (where } k > \tau)$$


 Fig. 10. FWHM vs. PZ  $\tau$  time constant.

2 mm rms) and time  $t_o$  of interaction. Then this information is processed by the tracking algorithm [1] to establish the interaction order. Only the results of tracking are saved on disk. This mode of operation performs substantial data compression and is referred to as “Mode 1”. It is also possible to operate the system, with software reconfiguration, in other modes.

The flow of GRETINA data is essentially from left to right and is represented by lines with arrowheads at one end (Fig. 11). This flow is implemented using TCP/IP sockets. Control and monitoring connections are more randomly oriented and are represented by filled circles at the ends. They are implemented using EPICS process variables (PVs) over epics channel access (CA). Connectors with diamond ends represent disk file access and connectors with plain ends are electronic links described in the previous section.

The set of octagons labeled DAQ represent the readout CPUs, one for each Ge crystal in the array. Each readout computer is a Motorola MVME5500 CPU module, running the VxWorks operating system, which reads out the data from four GRETINA digitizer modules over the VME bus. Each digitizer module has 10 channels and has a one-megabyte FIFO memory to allow readout of a continuous stream of data. The readout computer begins the process of crystal event building by time-sorting the

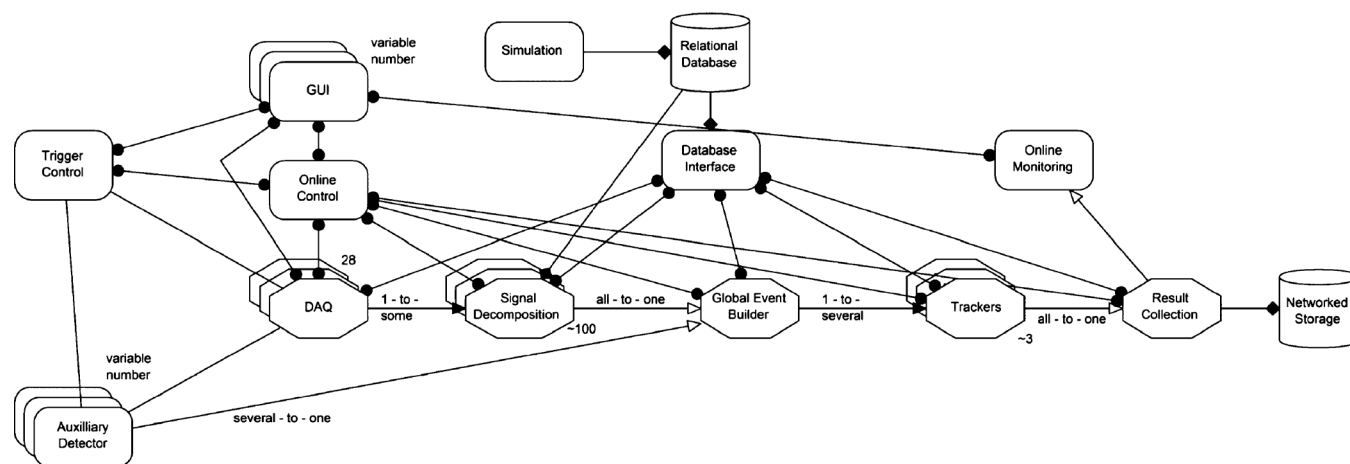


Fig. 11. Computing system high level block diagram.

data packets provided by the digitizers so that all segment events in a given crystal event will be contiguous in the data stream. The data stream is sliced into chunks separated by time gaps and these chunks are served up on demand to the next node in the pipeline, which in Mode 1 operation is an SD program. This sort of on-demand data server is indicated by the open arrowheads in the diagram. In addition, the readout CPUs support control and monitoring of the configuration of the electronics.

The SD algorithm is estimated to use over 99% of the computer power in the entire system; it is performed in the processor farm, which run signal decomposition nodes shown to the right of the DAQ nodes (for a description of one of these algorithms, refer to [8]). Each octagon represents one instance of the SD program, of which at least two are necessary to keep up with the requirement that the system must process 20 000 gamma/s (30 000 crystal interaction/s). These programs run on the processor farm. Each SD program has eight processing threads performing separate instances of the SD algorithm in parallel. The static data required for SD on a given crystal is almost two gigabytes resident in the server RAM. A single SD program can utilize 99% of the server CPU time and can typically process 600 interactions per second. Our server cluster has 62 nodes of which 56 can be devoted to SD. In practice two SD programs, working with data from different readout computers, are typically operated on each server to achieve better load-balancing in the cluster.

In this configuration, four SD programs compete to obtain data from each readout CPU and anywhere from 0 to 32 cores may be servicing a given crystal at any moment.

The outputs of the SD programs are sent to the global event builder (GEB), a single program which operates a receiver thread for the positions from each signal decomposition program. The primary function of the GEB is to gather the position, energy and timing data from all the detectors into a single time-ordered data stream. The GEB is also required to accept data from auxiliary detectors which may vary from experiment to experiment. The library provided for sending data to the GEB from such detectors is used by the SD program as well. The GEB provides a data stream in which the type, size

and timestamp of each data packet are indicated in a header. This entire data stream is sent to the tracker.

The track program examines data from similar times but different crystals, and multiple interaction points within single crystals in order to determine the probable order and gamma membership of individual interactions. The procedure used for sequencing the interactions is based on Compton scattering [1]. The results are saved to disk. The tracking program is multi-threaded in the same course-grained fashion as the SD program, with the result that the outputs need to be time-ordered before being stored.

As was mentioned earlier, Fig. 11 illustrates Mode 1 of operation. This is the mode for which the computing cluster and network infrastructure of GRETINA was designed. One major advantage of SD is that it reduces the magnitude of the data stream by a factor of approximately 30. GRETINA specifications require that each readout CPU be able to provide 10 MB/second of raw data. This results in an integrated network load of approximately 300 MB/s, or almost 3 Gb/s, on the network link between the network switch in the electronics shack and that in the server room. This link is 10 Gb/s; all other network interfaces in the system are 1 Gb/s. The data rate to disk is less than 20 MB/s, about one-third of what the GRETINA RAID arrays can sustain.

Other modes of operation are supported by reconfiguring the software. Which software runs on each node of the cluster is controlled by EPICS PVs interpreted by an EPICS finite-state machine program launcher. Each program (e.g., SD or GEB) is launched in the context of a telnet server that allows access to the program console for debugging purposes. All programs are also, at the top level, finite state machine based, and parameters that might normally be passed to programs on the command line or by environment variable in a batch environment are passed by EPICS PVs. A set of graphic user interfaces (GUIs) is provided to allow setting all these configurations interactively.

Specifically, Mode 3 was very useful in the engineering runs. The mode, in addition to saving the data after the SD and tracking, also saves the raw data. In this case one can compare the performance of the on- and off-line analysis.

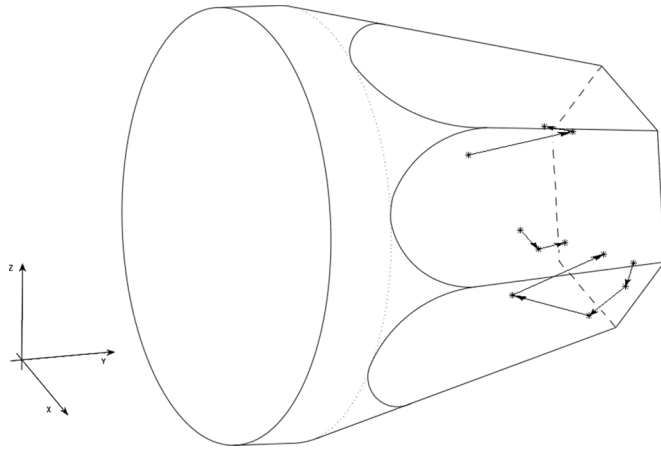


Fig. 12. Processed tracks inside the Ge crystal.

During each run data is written in a separate directory. Various auxiliary information including digitizer configuration and run start and stop times are saved as well.

#### IV. SYSTEM PERFORMANCE

In the 2nd quarter of 2011 a series of engineering runs were carried out to characterize the performance of GRETINA as a system. These tests took place in Cave 4C of the 88 Inches Cyclotron at LBNL. We will now present some of these results. Fig. 12 shows an example of the tracking algorithm reconstructing three good tracks. The algorithm interconnected a total of 11 gamma-ray interactions within the germanium crystal. Observe that one interaction starts on the front of the detector (the one toward the bottom of the drawing), then scatters to the back of the detector, and eventually scatters back to the front (the arrows show the sequence of the interactions).

A second experiment relies on the position resolution performance of the SD algorithm (approximately 2 mm rms). For a class of experiments, when the detected gamma-rays are emitted by a fast-moving source (e.g., experiments with heavy ion beams), the gamma-rays have a Doppler energy shift. The Doppler Effect correction is described by (1), where  $E_\gamma$  is the corrected energy,  $E_{\gamma_0}$  is the energy of the detected gamma-ray,  $V$  is the velocity of the beam used in the experimental setup (in this case non-relativistic),  $c$  is the speed of the light and  $\theta$  is the angle of emission defined by the beam path and a line between the gamma-ray source (i.e., the target) and the first interaction point in the Ge crystal [2].

$$E_\gamma = E_{\gamma_0} \left( 1 + \frac{V}{c} \cos \theta \right) \quad (1)$$

More important perhaps is the broadening of the gamma-ray line due the finite detector solid angle. This is illustrated in Fig. 13 that shows the results of the energy spectra with and without Doppler correction for  $^{84}\text{Kr} + ^{12}\text{C}$  fusions when tracking four interactions. The raw data peak corresponding to the two peaks highlighted by the arrows are centered on channel 1900. Observe the importance of accurately determining the angle  $\theta$  to

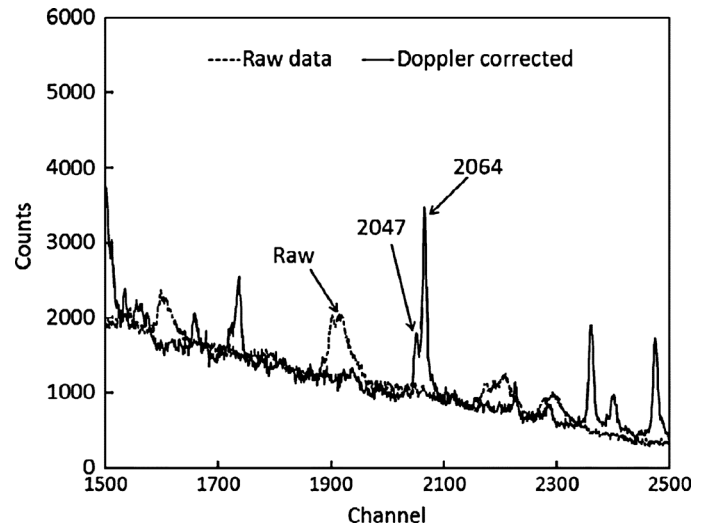


Fig. 13. Doppler Effect correction.

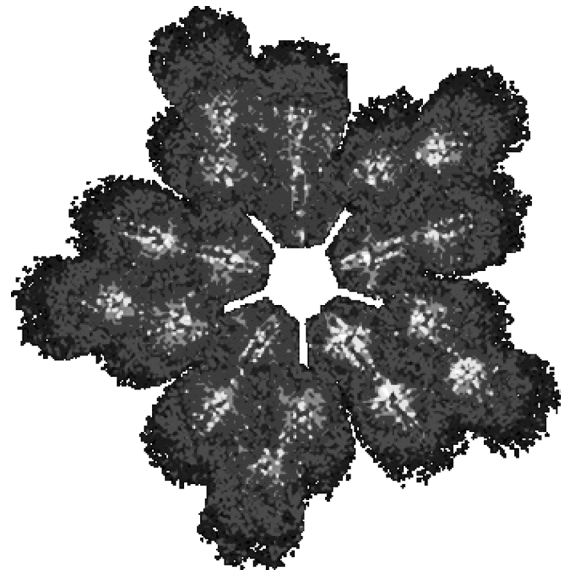


Fig. 14. Interaction of the gamma-rays with the germanium crystals.

correct not only the Doppler shift but also the Doppler broadening.

The last result presented here is the front view of the interaction of the gamma-rays with the germanium crystals. Fig. 14 shows the interaction of all gamma-rays with five detector modules, or 20 crystals, assembled in the support structure as shown in Fig. 5. The white or lighter dots represent more density of gamma-rays interactions, while darker gray or black represents less. One can observe that the front of the crystals detects more gamma-rays than the back.

#### ACKNOWLEDGMENT

The authors would like to thank I-Yang Lee and Augusto Macchiavelli for their valuable comments as well as the GRETINA team that carried out the engineering runs, in particular Heather Crawford for providing some of the results shown here, and Bryan Holmes for doing some of the drawings.

## REFERENCES

- [1] I. Y. Lee, "Gamma-ray tracking detectors," *Nucl. Instrum. Methods Phys. Res. A*, vol. 422, pp. 195–200, Feb. 1999.
- [2] M. A. Deleplanque *et al.*, "GRETA: Utilizing new concepts in  $\gamma$ -ray detection," *Nucl. Instrum. Methods Phys. Res. A*, vol. 430, pp. 292–310, July 1999.
- [3] F. S. Goulding and D. A. Landis, , J. Cerny, Ed., "Semiconductor detector spectrometer electronics," in *Nuclear Spectroscopy and Reactions*. New York: Academic, 1974, pt. A, pp. 413–481.
- [4] "The future of gamma-ray spectroscopy: GRETA, the gamma-ray energy tracking," [Online]. Available: [fsunuc.physics.fsu.edu/~gretina/GRETA\\_WP\\_Jan07\\_4.pdf](http://fsunuc.physics.fsu.edu/~gretina/GRETA_WP_Jan07_4.pdf), Dec. 2006
- [5] J. Anderson, R. Brito, D. Doering, T. Hayden, B. Holmes, J. Joseph, H. Yaver, and S. Zimmermann, "Data acquisition and trigger system for the gamma ray energy tracking in-beam nuclear array (GRETINA)," *IEEE Trans. Nucl. Sci.*, vol. 56, no. 1, pp. 258–265, Feb. 2009.
- [6] M. Cromaz *et al.*, "A digital signal processing module for gamma-ray tracking detectors," *Nucl. Instrum. Methods Phys. Res. A*, vol. 597, no. 2/3, pp. 233–237, 2008, doi:10.1016/j.nima.2008.07.137.
- [7] V. T. Jordanov and G. F. Knoll, "Digital synthesis of pulse shapes in real time for high resolution radiation spectroscopy," *Nucl. Instrum. Methods Phys. Res. A*, vol. 345, pp. 337–345, Jun. 1994.
- [8] S. Zimmermann and D. Doering, "Efficient gamma-ray signal decomposition analysis based on orthonormal transformation and fixed poles," in *Proc. Int. Conf. Acoustics, Speech, and Signal Processing*, Dallas, TX, Mar. 14–19, 2010.